The *Homo floresiensis* cranium (LB1): Size, scaling, and early *Homo* affinities

Adam D. Gordon*, Lisa Nevell, and Bernard Wood

Department of Anthropology, Center for the Advanced Study of Hominid Paleobiology, The George Washington University, 2110 G Street Northwest, Washington, DC 20052

Edited by David Pilbeam, Harvard University, Cambridge, MA, and approved February 8, 2008 (received for review October 22, 2007)

The skeletal remains of a diminutive small-brained hominin found in Late Pleistocene cave deposits on the island of Flores, Indonesia were assigned to a new species, *Homo floresiensis* [Brown P, *et al.* (2004) A new small-bodied hominin from the Late Pleistocene of Flores, Indonesia. *Nature* 431: 1055–1061]. A dramatically different interpretation is that this material belongs not to a novel hominin taxon but to a population of small-bodied modern humans affected, or unaffected, by microcephaly. The debate has primarily focused on the size and shape of the endocranial cavity of the type specimen, LB1, with less attention being paid to the morphological evidence provided by the rest of the LB1 cranium and postcranium, and no study thus far has addressed the problem of how scaling would affect shape comparisons between a diminutive cranium like LB1 and the much larger crania of modern humans. We show that whether or not the effects of its small cranial size are accounted for, the external cranial morphology of the LB1 cranium cannot be accommodated within a large global sample of normal modern human crania. Instead, the shape of LB1, which is shown by multivariate analysis to differ significantly from that of modern humans, is similar to that of *Homo erectus sensu lato*, and, to a lesser extent, *Homo habilis*. Our results are consistent with hypotheses that suggest the Liang Bua specimens represent a diminutive population closely related to either early *H. erectus s. l.* from East Africa and/or Dmanisi or to *H. habilis*.

allometry | hominin phylogeny

Most studies that have addressed the taxonomic affinities of the Liang Bua hominin material have focused on the size and morphology of the endocranial cavity of LB1 (1–8) and on the postcranium, particularly the forelimb (9, 10). Relatively little analysis has addressed the external morphology of the skull and dentition. On the basis of univariate assessments of categorical and metric variables, the describers of the Ling Bua specimens showed that there was a dissimilarity between LB1 and modern humans and a general similarity between LB1 and *H. erectus sensu lato* (11) (hereafter referred to as *H. erectus*). In contrast, others reported that 94 descriptive features of the cranium of LB1 all fell within the range for normal, nonpathological modern humans (12). The original report included a multivariate principal components analysis (PCA) of five cranial vault measurements taken on LB1, one modern human and several fossil hominins (11). In that analysis, LB1 shape was found to be most similar to *H. erectus* as represented by KNM-ER 3883, KNM-ER 3733, and Sangiran 2. However, in a subsequent multivariate canonical variates analysis (CVA) of several cranial measurements for LB1, normal modern humans, two microcephalic modern humans, chimpanzees, and fossil hominins, other researchers (13) concluded that LB1 is distinct from all hominins, including *H. erectus*. Thus, no consensus has emerged about what the external cranial morphology can tell us about the affinities of the LB1 cranium.

It is recognized by researchers on all sides of the debate that LB1 has an extremely small endocranial volume (and thus presumably had a small brain) relative to its body size (1, 3–7, 11, 12, 14). Scaling relationships have been considered with regard to endocranial size (as it scales with body size) (3, 5, 6, 11) and brain component size (as they scale with endocranial size) (14), but, to date, no study has considered the scaling of cranial vault shape and cranial size when assessing morphological similarity between LB1, modern humans, and fossil hominins. Because the LB1 cranium is so small relative to modern humans and most fossil *Homo*, morphological analyses must take into account how cranial shape scales with cranial size because this relationship may not be isometric. However, care must be taken when doing this, because LB1 falls well outside the size range used to generate regression slopes.

Here, we address two specific questions regarding the external shape of the LB1 cranium: (*i*) Can LB1 cranial shape be accommodated within the range of cranial shape of a worldwide sample of normal, nonpathological, modern humans? (*ii*) If not, then which hominin taxon or subset of hominin crania does LB1 most resemble? In investigating both of these questions, we use two approaches, one of which assumes that cranial shape is unaffected by overall cranial size (isometry), and the other of which uses the comparative sample(s) (extant and fossil) to identify empirical scaling relationships. It has been suggested that the microcephalic crania included in previous cranial shape analyses are inappropriate as comparators for LB1 because they are either not fully adult or because they have relatively high cranial capacities (5, 6). In any event, microcephaly can result from a variety of syndromes (15) resulting in a range of phenotypes (7, 16). This makes it unlikely that any small comparative sample will adequately represent the possible range of morphologic variation present in microcephalic crania. Consequently, we limit our analyses to nonpathological specimens, but, when we discuss the results of our comparisons with fossil hominins, we address the likelihood of the hypothesis that the LB1 cranium is an example of a microcephalic modern human.

Results and Discussion

Data for six cranial vault variables were collected from the literature for LB1 (11), a worldwide sample of 2,524 adult recent modern humans (17), and for 30 fossil hominin crania (11, 18–27) (see *Materials and Methods* and supporting information (SI) Table S1). Univariate comparisons of size-adjusted shape variables between LB1 and the modern human sample yield mixed results: LB1 does not differ significantly from the modern comparative sample in size-adjusted cranial length (GOL′), maximum cranial breadth (XCB′), or cranial base length (BNL′) (see *Materials and Methods*), whereas it does differ significantly in size-adjusted cranial height (BBH′), maxillary prognathism (BPL′), and biasterionic breadth

Author contributions: A.D.G. and L.N. contributed equally to this work; A.D.G., L.N., and B.W. designed research; A.D.G., L.N., and B.W. performed research; A.D.G. and L.N. analyzed data; A.D.G., L.N., and B.W. wrote the paper.

The authors declare no conflict of interest.

This article is a PNAS Direct Submission.

*To whom correspondence should be addressed. E-mail: adam.d.gordon@gmail.com.

This article contains supporting information online at www.pnas.org/cgi/content/full/0710041105/DCSupplemental.

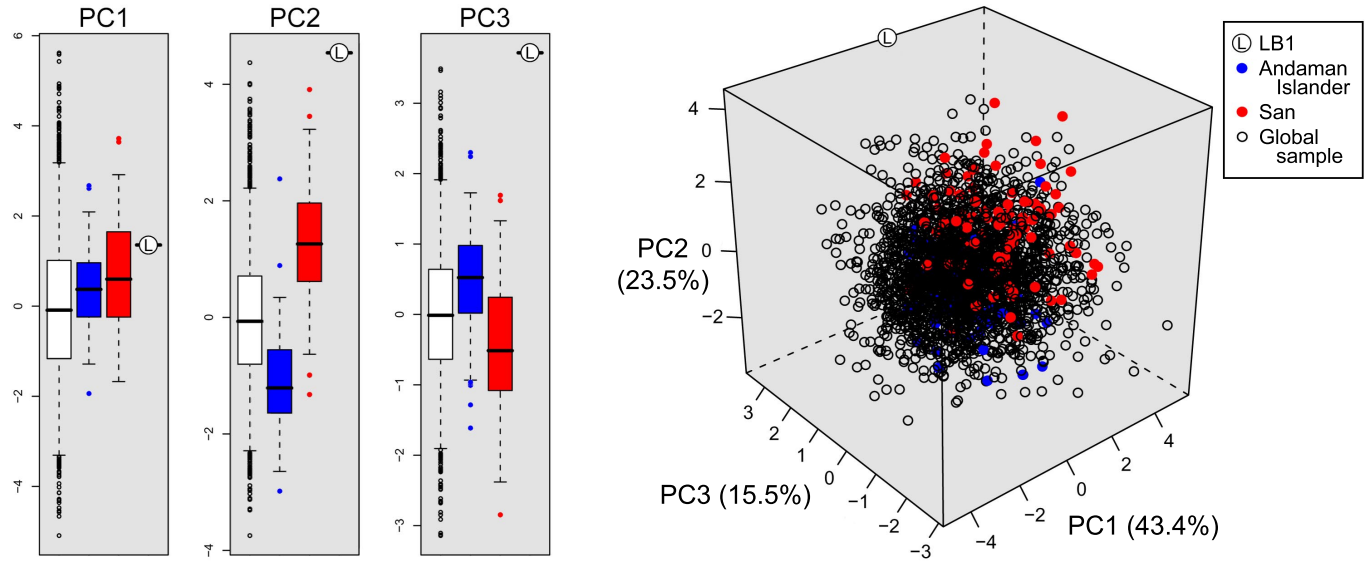

Fig. 1. Box-and-whisker plots and 3D plot of the first three principal components for a PCA of six shape variables for the recent modern human comparative sample and LB1. Boxes indicate first and third quartiles, whiskers extend to the most extreme data point that is no more than a single interquartile range from the box, and more extreme values are shown as individual data points. Cranial shape in LB1 differs from the PCA centroid for modern humans by >4.5 standard deviations regardless of whether allometric scaling relationships within modern humans are either ignored (shown here) or taken into account (see *Results and Discussion*).

(ASB′) (*t* tests, $\alpha = 0.05$). Values are within the modern human range for all shape variables except relative cranial height, for which LB1 has a value lower than that of all 2,524 crania in our modern human sample. However, multivariate consideration of these variables demonstrates that the combination of values present in LB1 is distinct from all modern humans.

Plots of the first three principal components in an analysis of logged shape variables show a tight cluster for the modern human crania that excludes LB1 (Fig. 1). In contrast to the placement of LB1 outside the modern human cluster, the two modern human populations with the smallest crania (Andaman Islanders and San) cluster in the middle of the range of principal component (PC) 1 and span most of the ranges of PCs 2 and 3 (Fig. 1). The placement of these two populations shows that size plays a negligible role in the morphological separation of crania in this analysis. When considering all six principal components,

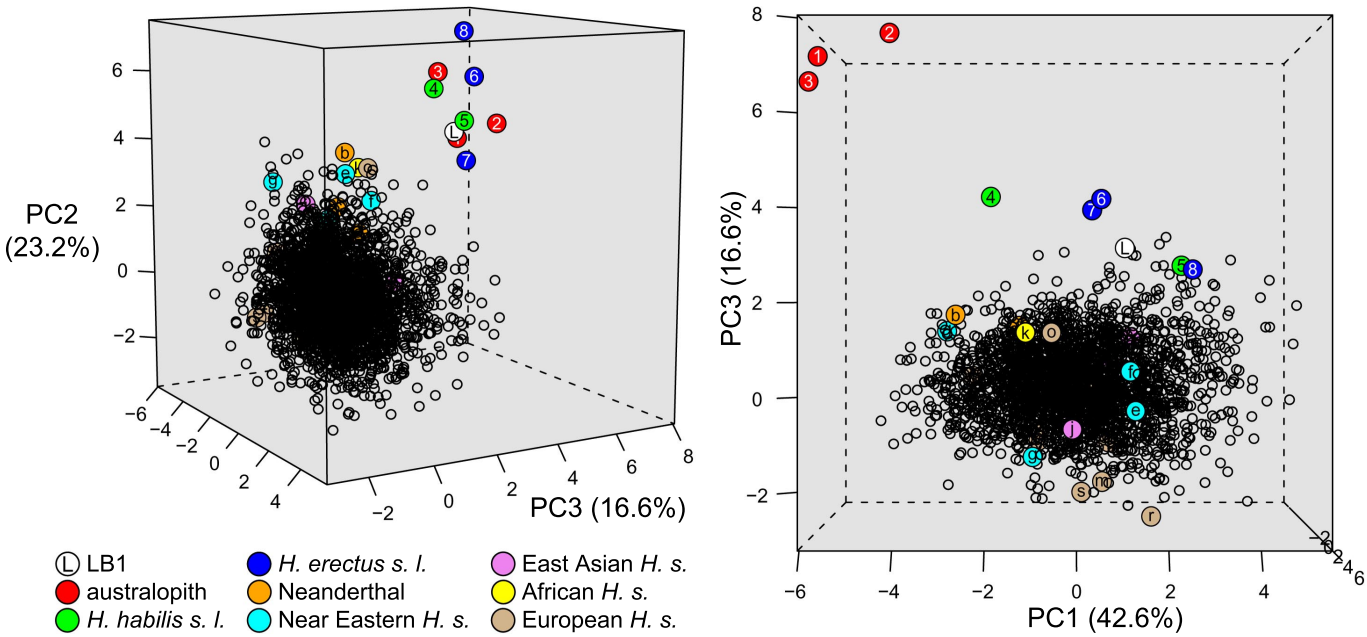

Fig. 2. 3D plot of the first three principal components for a PCA of six shape variables for all modern and extinct specimens. Symbols are as follows: open circles, recent modern humans; L, LB1; 1, Sts 5; 2, KNM-ER 406; 3, OH 5; 4, KNM-ER 1813; 5, OH 24; 6, KNM-ER 3733; 7, D2700; 8, Sangiran 17; a, La Ferrassie; b, La Chapelle; c, Shanidar 1; d, Qafzeh 6; e, Skhul 4; f, Skhul 5; g, Skhul 9; h, Minatogawa 1; i, Minatogawa 4; j, ZUC 101; k, Kabwe; l, Abri Pataud; m, Cro-Magnon 1; n, Dolni Vestonice; o, Gibraltar; p, Kaufertsberg; q, Mladec 1; r, Oberkassel 1; s, Oberkassel 2; t, Ofnet 6; u, Ofnet 13; v, Ofnet 24. Note that fossil *H. sapiens* and Neanderthals plot within or on the periphery of the modern human cluster and that the remaining fossils are shifted away from the modern human cluster in the same general direction for PC2 (elevation in the plot at *Left*) and PC3 (elevation in the plot at *Right*). LB1 is closest to D2700 and KNM-ER 3733.

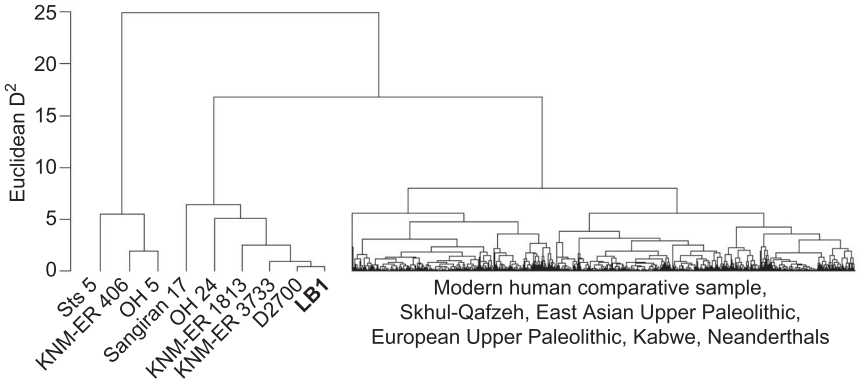

Fig. 3. WPGMA cluster analysis based on squared Euclidean distances. Note that australopiths (Sts 5, KNM-ER 406, OH 5) cluster to the exclusion of the genus *Homo*, *Paranthropus boisei* specimens cluster to the exclusion of *Australopithecus africanus*, and LB1 clusters with earlier members of the genus *Homo* to the exclusion of archaic and modern *Homo sapiens* and Neanderthals.

using Euclidean distance, LB1 is the most distant specimen from the modern human centroid. A randomized *t* test of Euclidean distance from the modern human centroid shows a highly significant difference between LB1 and the comparative sample, with LB1 cranial shape differing from the modern human centroid by 4.52 standard deviations ($P < 0.001$).

When fossil crania are included in the PCA, fossil *H. sapiens* and Neanderthals plot within or on the periphery of the modern human cluster and the remaining fossil hominin crania are shifted away from the modern human cluster in shape space in the same general direction as each other; i.e., morphologies that distinguish each fossil from modern humans may differ among the fossils in degree but not overall morphological trajectory (e.g., to a greater or lesser degree the fossil crania tend to have relatively shorter cranial vaults and greater maxillary prognathism than the modern humans) (Fig. 2). LB1 is morphologically similar to the *H. erectus* specimens, particularly KNM-ER 3733 and D2700. This relationship is supported by a weighted pair-group method of arithmetic means (WPGMA) cluster analysis (28) based on the squared Euclidean distances between specimens for the six principal components (Fig. 3). Three major clusters emerge: all of *Homo* groups to the exclusion of the australopiths, and later *Homo* (*H. sapiens*, Neanderthals) groups to the exclusion of earlier *Homo* (*H. erectus*, *H. habilis*). LB1 is nested within the earlier *Homo* cluster. Fossil *H. sapiens* and Neanderthals are spread throughout the later *Homo* cluster and do not form a discrete, exclusive group.

This clustering pattern demonstrates that (*i*) although the six variables selected for this study do not sort hominin crania into species, crania are sorted in a manner that corresponds to conventional taxonomic interpretations; (*ii*) major morphological differences distinguish clusters; and (*iii*) when shape is considered in the absence of scaling patterns, LB1 appears most similar to the non-Asian *H. erectus* specimens D2700 (from Dmanisi, Georgia) and KNM-ER 3733 (from Koobi Fora, Kenya) and is distinct from later *Homo*. Furthermore, comparison of principal component Euclidean distances of LB1 from species/fossil group centroids shows that LB1 is closest to the centroid of non-Asian *H. erectus*, followed by the centroid of all *H. erectus* (including Sangiran 17) (Table 1). Likewise, when the mean distance of specimens from the group centroid is considered for each taxon or group of fossils, adding LB1 to a group decreases the mean distance only for *H. erectus* and non-Asian *H. erectus*. This indicates that the inclusion of LB1 in either of these groups reduces the overall morphological variance for the group as a whole, whereas it increases morphological variance if it is added to any other group (Table 1).

To assess the effects of scaling relationships on expected shape for crania as small as LB1, bivariate empirical scaling relationships

Table 1. Euclidean distances based on principal component scores for hominin groups and sum of squared residuals for LB1 from hominin bivariate regressions

Group	*N*	Distance, centroid to LB1	Mean distance to centroid without LB1	Mean distance to centroid with LB1	Sum of squared residuals of LB1 from fitted scaling lines	Sum of squared standardized residuals of LB1 from fitted scaling lines	Mean of absolute value of standardized residuals of LB1 from fitted scaling lines
Non-Asian *H. erectus*	2	0.534	**0.546**	**0.501**	0.007	15.7	1.38
H. habilis	2	1.578	1.146	1.190	0.008	12.8	1.21
H. erectus	3	0.591	**0.913**	**0.802**	0.011	22.3	1.68
All *Homo* fossils	27	1.766	1.547	1.559	0.017	30.3	1.76
All *Homo*	2,551	2.617	1.008	1.009	0.041	66.8	3.00
Recent modern humans	2,524	2.627	1	1.001	0.042	68.9	3.06
European fossil *H. s.*	11	2.688	1.065	1.211	0.096	157	4.73
Australopiths	3	3.864	1.149	1.855	0.104	172	4.89
Asian fossil *H. s.*	3	2.180	0.803	1.138	0.189	372	5.69
Neanderthals	3	1.989	0.581	0.948	0.356	763	9.84
Near East fossil *H. s.*	4	1.837	1.301	1.378	0.384	712	10.4

Distances were standardized such that a distance of 1 is equal to the mean distance of a recent modern human from the centroid of that group. LB1 residuals were standardized by the standard deviation of recent modern human residuals for each bivariate regression. Groups are sorted by the sum of squared residuals. Bold-faced type indicates that mean distance from each specimen to the group centroid decreases when LB1 is included in that group. *H. s.*, *Homo sapiens*.

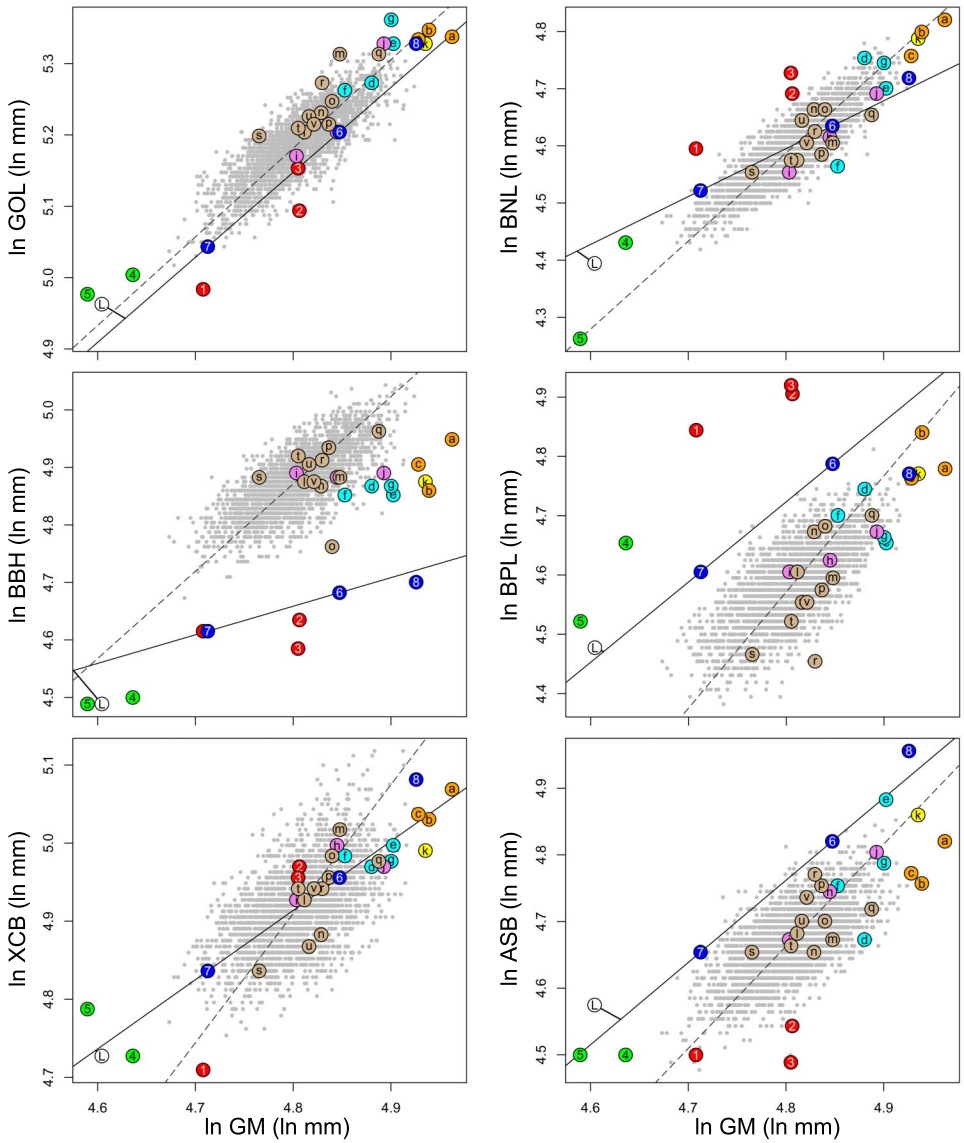

Fig. 4. Bivariate scaling relationships between cranial variables and overall cranial size (cranial GM) in recent modern humans (light gray points) and fossil hominins. Symbols for fossil specimens follow Fig. 2. Dashed lines are major axis fitted lines for the recent modern human sample; solid lines connect non-Asian *H. erectus* specimens (i.e., KNM-ER 3733 and D2700). The sum of squared residuals of LB1 from all six fitted lines is minimized when using the non-Asian *H. erectus* lines (residuals are calculated along the minor axis and are shown as thick solid lines in plots; see Table 1 and *Materials and Methods*). Regression slopes and confidence limits are provided in Table S2.

between the log of each of the six linear measurements and logged overall cranial size (measured as the geometric mean of all six measurements) were estimated by fitting major axis lines for the modern human sample and for each of the fossil taxa (Fig. 4). Although sample sizes for the fossil groups were generally too small to generate meaningful statistical comparisons with isometric scaling relationships, scaling relationships could be determined for the modern human sample. Using major axis regression, all six modern human slopes were found to be significantly positively allometric (Table S2). When the modern human crania were scaled to the size of the LB1 cranium, randomized t tests for a PCA of size-adjusted shape variables for LB1 and scaled variables for modern humans show that LB1 cranial shape is even more distinct from modern human cranial shape when scaling is taken into account, with LB1 differing from the centroid of scaled human shape by 4.82 standard deviations ($P < 0.001$). Clearly the cranial shape of LB1 cannot be accommodated within the range of shape present in nonpathological modern humans, regardless of whether scaling is taken into account.

Leaving aside for the moment the issue of pathology, the question remains that if LB1 does not resemble modern *H. sapiens*, does it resemble any other hominin taxon? As shown above, when scaling is not taken into account, LB1 external cranial shape closely resembles that of *H. erectus*, particularly non-Asian *H. erectus*. Similarly, a preliminary geometric morphometric analysis found that the neurocranium of LB1 is most similar to that of *H. erectus* (29). To identify the best fit between LB1 and scaled cranial shape in various fossil hominin groups, minor axis residuals of LB1 from estimated scaling relationships for each group were used to calculate sums of squared residuals for all six cranial variables. Sum of squared residuals are minimized by using *H. erectus* and *H. habilis* scaling patterns (based on both standardized and unstandardized residuals; see *Materials and Methods*), with the lowest overall sum of squared residuals found when Sangiran 17 is removed from *H.*

erectus and scaling relationships are based solely on KNM-ER 3733 and D2700 (Fig. 4 and Table 1). This result indicates that LB1 cranial shape is not particularly similar to the more derived cranial shape of Asian *H. erectus*, but rather it shares similarities with the less derived cranial morphologies of *H. habilis* and *H. erectus* from East Africa and Dmanisi. Likewise, the mandibles of LB1 and LB6/1 are reported to be morphologically more similar to non-Asian *H. erectus* mandibles than to those of *H. erectus* from Java and China (30).

With regard to microcephaly, it should be noted that in the shape analysis performed here, LB1 cranial shape is shown to differ significantly from the modern human comparative sample (and from fossil *H. sapiens* and Neanderthals) and to be very close in morphological space to non-Asian *H. erectus* specimens (D2700 and KNM-ER 3733) and *H. habilis* specimens (KNM-ER 1813 and OH 24). LB1 and the non-Asian *H. erectus* specimens are much closer than the average pairwise distance between modern human crania, and standardized residuals of LB1 from the estimated non-Asian *H. erectus* and *H. habilis* scaling relationships average 1.38 and 1.21 standard deviations away from expected shape, respectively (as opposed to >3 standard deviations from expected shape for modern humans), well within the range of population-level variation (Table 1). Thus, if microcephaly is responsible for the extremely small size of the LB1 cranium, of all possible ways that microcephaly could cause LB1 cranial shape to differ from that of modern humans for these six variables, it happens to differ in the same way that earlier *Homo* species differ from modern humans.

Assuming that LB1 is not pathological, what do the results of this study imply for the taxonomy and phylogeny of this specimen? Based on the work reported here, the original describers of this material are justified in not attributing LB1 to *H. sapiens*, and our results are consistent with the introduction of a new species, *H. floresiensis* (11), or with the hypothesis that the Liang Bua material represents a population of diminutive, small-brained *H. erectus* (S. Antón in ref. 31).

As for phylogeny, those who support the erection of a new taxon have developed several possible scenarios, including that (*i*) *H. floresiensis* is the product of insular dwarfing of *H. erectus* on Flores or nearby islands (11), (*ii*) *H. floresiensis* and *H. erectus* shared a recent common ancestor (1, 4, 32), or (*iii*) *H. floresiensis* is descended from *Australopithecus* via a lineage distinct from that of *H. erectus* (4, 30). Studies of the postcranial skeleton of LB1 show that the forelimb is primitive with respect to modern humans in the carpals (10) and humerus (9, 30), and tend to support the evolution of *H. floresiensis* from *H. erectus* or an earlier taxon. Other than a partial lunate from Zhoukoudian, no carpals are known from *H. erectus*, but the LB1 carpals are very similar in overall morphology to those of *H. habilis* and *Australopithecus* (10). With respect to other postcranial evidence, the low degree of humeral torsion in LB1 is similar to that seen in the Dmanisi hominins (33), KNM-WT15000 (9), and australopiths (9).

The results of this study of external cranial morphology suggest that a close relationship between LB1 and australopiths is unlikely, but a close relationship with *H. habilis* cannot be ruled out. The LB1 cranium and the *H. erectus* specimens do not cluster to the exclusion of *H. habilis*, and the sum of standardized squared residuals for comparison of LB1 shape to scaled *H. habilis* is slightly lower than that for the comparison to scaled non-Asian *H. erectus* (Table 1). Given the similarity in postcranial material between LB1 and *H. habilis*, it is possible that LB1 may turn out to be even more similar in overall morphology to *H. habilis* than to *H. erectus.*

The results presented here are in broad agreement with phylogenetic scenarios suggesting that *H. floresiensis* is the product of insular dwarfing of *H. erectus* on Flores or nearby islands or that *H. floresiensis* and *H. erectus* shared a recent common ancestor, possibly *H. habilis*. The close morphological similarity between the LB1 cranium, D2700, and KNM-ER 3733 in conjunction with the lack of close similarity between these specimens and Sangiran 17 argues for an ancestry for LB1 that does not include later Asian *H. erectus*.

Materials and Methods

The cranial sample includes 2,524 adult recent modern humans, LB1, and 30 fossil hominin crania; crania are assigned to groups on the basis of taxonomy and geographic location (see Table S1). Six external cranial variables are considered for each specimen: cranial length [glabella-opisthocranion length (GOL)], cranial height [basion-bregma height (BBH)], maximum cranial breadth [euryon-euryon breadth (XCB)], cranial base length [basion-nasion length (BNL)], maxillary prognathism [basion-prosthion length (BPL)], and biasterionic breadth [asterion-asterion breadth (ASB)]. Shape variables are calculated by dividing each measurement by the geometric mean of all six measurements for a given specimen and are denoted by the prime symbol; e.g., GOL′ (34, 35).

Shape Analyses. Morphological difference between specimens is calculated as the Euclidean distance, using all six principal components generated by a PCA. Euclidean distance of PCA scores is preferred over Mahalanobis distance, because, although both measure distance using orthogonal axes, Mahalanobis distance rescales all variables to have equal variance, whereas Euclidean distance retains the variance structure of the variables, which in this case (principal components) are scaled to the proportion of variance they account for in the total dataset. Using distances based on PCA scores rather than on the shape variables themselves provides a measure of shape difference defined by the shape variation between specimens (dominated by the modern human sample) as opposed absolute shape differences, although results should be similar. In all cases, distances have been scaled such that the average distance of modern humans to their centroid equals 1.00. Randomized *t* tests are used to identify whether the distance of LB1 from the modern human centroid significantly exceeds the distance of modern humans from their centroid. Additionally, the distance of LB1 from the centroid of each fossil group is calculated to identify degree of morphological similarity. To assess the effect of LB1 on morphological variability within a group, two sets of distances are calculated: (*i*) mean distance of all members of a group from their own centroid and (*ii*) mean distance of all members of a group plus LB1 from their combined centroid.

Scaling Analyses. To determine how LB1 cranial shape compares to that of modern humans scaled down to the size of LB1, least squares regression lines are calculated for each logged cranial variable against the logged geometric mean of all cranial variables for the modern human sample; then, residuals from all 2,524 modern human crania are translated down the regression line to the geometric mean size of LB1 to predict the six measurements for each modern human if they were scaled to the size of LB1. Although classical calibration (i.e., swapping the variables on the *x* and *y* axes) may be preferred over the inverse calibration used here when extrapolating beyond the size range of the regression sample (36), using residuals to retain the proportional difference in cranial variables from expected values when predicting scaled cranial shape is only possible using inverse calibration. To compare LB1 to scaled shape expectations more broadly for both modern and fossil crania, bivariate scaling relationships with overall cranial size were estimated by using major axis line fits for fossil and modern crania. These line fits were not used in significance tests of regression parameters as the fossil group sample sizes are generally too low for such tests (in some cases, only two specimens, with zero degrees of freedom), but rather as simple estimates for observed scaling relationships present in a sample of fossil crania. Minor axis residuals of LB1 from estimated scaling lines were squared and summed to produce a measure of morphological dissimilarity of LB1 from expected cranial shape for each group/taxon. Additionally, residuals were standardized by dividing by the standard deviation of the 2,524 residuals for the modern human regression for each of the six cranial variables (e.g., the residual of LB1 from the fitted major axis line of GOL versus cranial GM for australopiths was divided by the standard deviation of modern human residuals from the fitted major axis line of GOL versus cranial GM for modern humans). Sums of standardized residuals were calculated and means for absolute values of standardized residuals. These values were compared among groups, with the lowest values indicating greatest morphological similarity between LB1 and the expected shape for a particular group as determined by the estimated scaling patterns.

ACKNOWLEDGMENTS. The authors thank the editor and two anonymous reviewers. This work was supported by George Washington University's Academic Excellence Program (A.D.G., L.N., and B.W.), National Science Foundation Integrative Graduate Education and Research Traineeship 9987590 (L.N.), and a George Washington University University Professorship (B.W.).

1. Falk D, *et al.* (2005) The brain of LB1, *Homo floresiensis. Science* 308:242–245.
2. Falk D, *et al.* (2005) Response to comment on ''The brain of LB1, *Homo floresiensis*.'' *Science* 310:236c.
3. Falk D, *et al.* (2006) Response to comment on ''The brain of LB1, *Homo floresiensis*.'' *Science* 312:999c.
4. Falk D, *et al.* (2007) Brain shape in human microcephalics and *Homo floresiensis. Proc Natl Acad Sci USA* 104:2513–2518.
5. Martin RD, Maclarnon AM, Phillips JL, Dobyns WB (2006) Flores hominid: New species or microcephalic dwarf? *Anat Rec A* 288A:1123–1145.
6. Martin RD, *et al.* (2006) Comment on ''The brain of LB1, *Homo floresiensis*.'' *Science* 312:999b.
7. Richards GD (2006) Genetic, physiologic and ecogeographic factors contributing to variation in *Homo sapiens*: *Homo floresiensis* reconsidered. *J Evol Biol* 19:1744–1767.
8. Weber J, Czarnetzki AE, Pusch CM (2005) Comment on ''The brain of LB1, *Homo floresiensis*.'' *Science* 310:236b.
9. Larson SG, *et al* (2007) *Homo floresiensis* and the evolution of the hominin shoulder. *J Hum Evol* 53:718–731.
10. Tocheri MW, *et al.* (2007) The primitive wrist of *Homo floresiensis* and its implications for hominin evolution. *Science* 317:1743–1745.
11. Brown P, *et al* (2004) A new small-bodied hominin from the Late Pleistocene of Flores, Indonesia. *Nature* 431:1055–1061.
12. Jacob T, *et al.* (2006) Pygmoid Australomelanesian *Homo sapiens* skeletal remains from Liang Bua, Flores: Population affinities and pathological abnormalities. *Proc Natl Acad Sci USA* 103:13421–13426.
13. Argue D, Donlon D, Groves C, Wright R (2006) *Homo floresiensis*: Microcephalic, pygmoid, *Australopithecus*, or *Homo*? *J Hum Evol* 51:360–374.
14. Conroy GC, Smith RJ (2007) The size of scalable brain components in the human evolutionary lineage: With a comment on the paradox of *Homo floresiensis. Homo* 58:1–12.
15. Gilbert SL, Dobyns WB, Lahn BT (2005) Genetic links between brain development and brain evolution. *Nat Rev Genet* 6:581–590.
16. Richards GD (1985) Analysis of a microcephalic child from the late period (c. 1100–1700 AD) of central California. *Am J Phys Anthropol* 68:343–357.
17. Howells WW (1996) Howells' craniometric data on the internet. *Am J Phys Anthropol* 101:441–442.
18. Heim JL (1989) A new reconstruction of the Chapelle-aux-Saints cranium: Method and results. *Bull Mem Soc d'Anth Paris* 1:95–118.
19. Kidder JH (1996) Defining anatomically modern *Homo sapiens* in the context of modern human origins: A size and shape approach. Ph.D. Thesis (University of Tennessee, Nashville, TN).
20. Lahr MM (1996) *The Evolution of Human Diversity* (Cambridge Univ Press, Cambridge).
21. Lordkipanidze D, *et al.* (2006) A fourth hominin skull from Dmanisi, Georgia. *Anat Rec A* 288A:1146–1157.
22. McCown TD, Keith A (1939) *The Stone Age of Mount Carmel II: The Fossil Human Remains from the Levalloiso-Mousterian* (Clarendon, Oxford).
23. Suzuki H (1982) in *The Minatogowa Man: The Upper Pleistocene Man from the Island of Okinawa*, eds Suzuki H, Hanihara K (Univ of Tokyo Press, Tokyo), pp 7–49.
24. Tobias PV (1967) *Olduvai Gorge. Volume 2: The Cranium and Maxillary Dentition of Australopithecus (Zinjanthropus) boisei* (Cambridge Univ Press, Cambridge).
25. Trinkaus E (1983) *The Shanidar Neanderthals* (Academic, New York).
26. Wood BA (1991) *Koobi Fora Research Project. Volume 4: Hominid Cranial Remains* (Clarendon, Oxford).
27. Wu X, Zhang Z (1985) in *Paleoanthropology and Palaeolithic Archaeology in the People's Republic of China*, eds Wu R, Olsen JW (Academic, Orlando), pp 107–133.
28. Sneath PHA, Sokal RR (1973) *Numerical Taxonomy: The Principles and Practice of Numerical Classification* (W. H. Freeman, San Francisco).
29. Baab K, McNulty K, Brown P (2007) Allometric scaling of craniofacial shape: Implications for the Liang Bua hominins. *PaleoAnthropology* 2007:A2.
30. Morwood MJ, *et al.* (2005) Further evidence for small-bodied hominins from the Late Pleistocene of Flores, Indonesia. *Nature* 437:1012–1017.
31. Wong K (2005) The littlest human. *Sci Am* 2(292):56–65.
32. Groves C (2004) Some initial informal reactions to publication of the discovery of *Homo floresiensis* and replies from Brown & Morwood. *Before Farming* 4:2.
33. Lordkipanidze D, *et al.* (2007) Postcranial evidence from early *Homo* from Dmanisi, Georgia. *Nature* 449:305–310.
34. Jungers WL, Falsetti AB, Wall CE (1995) Shape, relative size, and size-adjustments in morphometrics. *Yrbk Phys Anthropol* 38:137–161.
35. Mosimann JE (1970) Size allometry: size and shape variables with characterizations of the lognormal and generalized gamma distributions. *J Amer Stat Assoc* 65:930–945.
36. Konigsberg LW, Hens SM, Jantz LM, Jungers WL (1998) Stature estimation and calibration: Bayesian and maximum likelihood perspectives in physical anthropology. *Year Book Phys Anthropol* 41:65–92.

Supporting Information

Gordon *et al.* 10.1073/pnas.0710041105

Supporting References

1. Brown P, *et al.* (2004) A new small-bodied hominin from the Late Pleistocene of Flores, Indonesia. *Nature* 431: 1055–1061.
2. Howells WW (1996) Howells' craniometric data on the internet. *Am J Phys Anthropol* 101: 441–442.
3. Wood BA (1991) *Koobi Fora Research Project. Volume 4: Hominid Cranial Remains* (Clarendon, Oxford).
4. Tobias PV (1967) *Olduvai Gorge. Volume 2: The Cranium and Maxillary Dentition of Australopithecus (Zinjanthropus) boisei* (Cambridge Univ Press, Cambridge).
5. Lordkipanidze D, *et al.* (2006) A fourth hominin skull from Dmanisi, Georgia. *Anat Rec A* 288A:1146–1157.
6. Heim JL (1989) A new reconstruction of the Chapelle-aux-Saints cranium: Method and results (in French). *Bull Mem Soc d'Anth Paris* 1:95–118.
7. Kidder JH (1996) Defining anatomically modern *Homo sapiens* in the context of modern human origins: A size and shape approach. Ph.D. Thesis, University of Tennessee, Nashville, TN.
8. Trinkaus E (1983) *The Shanidar Neanderthals* (Academic, New York).
9. Suzuki H (1982) in *The Minatogowa Man: The Upper Pleistocene Man from the Island of Okinawa*, eds Suzuki H, Hanihara K (Univ of Tokyo Press, Tokyo), pp 7–49.
10. Lahr MM (1996) *The Evolution of Human Diversity* (Cambridge Univ Press, Cambridge, UK).
11. Wu X, Zhang Z (1985) in *Paleoanthropology and Palaeolithic Archaeology in the People's Republic of China*, eds Wu R, Olsen JW (Academic, Orlando), pp 107–133.
12. McCown TD, Keith A (1939) *The Stone Age of Mount Carmel II: The Fossil Human Remains from the Levalloiso-Mousterian* (Clarendon, Oxford).

Table S1. Cranial measurements

Specimen (ref.)	Species	GOL	BBH	XCB	BNL	BPL	ASB
LB1 (1)	—	143	89	113	81	88	97
2,524 crania (2)	Recent *H. sapiens*	151–206	107–155	116–167	83–120	80–123	88–128
KNM-ER 406 (3)	*P. boisei*	163	103	144	109	135	94
OH 5 (4)	*P. boisei*	173	98 (3)	142	113	137	89
Sts 5 (3)	*A. africanus*	146	101	111	99	127	90
KNM-ER 1813 (3)	*H. habilis*	149	90	113	84	105	90
OH 24 (3)	*H. habilis*	145	89	120	71	92	90
D2700 (5)	*H. erectus*	155	101	126	92	100	105
KNM-ER 3733 (3)	*H. erectus*	182	108	142	103	120	124
Sangiran 17 (3)	*H. erectus*	206	110	161	112	118	142
La Chapelle (6)	*H. neanderthalensis*	210	129	153	121.4	126.5	116.4
La Ferrassie (7)	*H. neanderthalensis*	208	141	159	124	119	124
Shanidar 1 (8)	*H. neanderthalensis*	207.2	135	154	116.4	117.1	118.2
Kabwe (7)	*H. sapiens* (African)	206	131	147	120	118	129
Minatogawa 1 (9)	*H. sapiens* (Asian)	182	132 (10)	148	101	102	115
Minatogawa 4 (9)	*H. sapiens* (Asian)	176	133 (10)	138	95	100	107
ZUC 101 (11)	*H. sapiens* (Asian)	206	133	144	109	107	122
Abri Pataud (7)	*H. sapiens* (European)	182	131	138	97	100	108
Cro-Magnon 1 (7)	*H. sapiens* (European)	203	132	151	100	99	107
Dolni Vestonice (7)	*H. sapiens* (European)	187	130	132	106	107	105
Gibraltar (12)	*H. sapiens* (European)	190	117	146	106	108	110
Kaufertsberg (7)	*H. sapiens* (European)	184	139	142	98	97	116
Mladec 1 (7)	*H. sapiens* (European)	203	143	145	105	110	112
Oberkassel 1 (7)	*H. sapiens* (European)	195	136	140	102	86	118
Oberkassel 2 (7)	*H. sapiens* (European)	181	132	126	95	87	105
Ofnet 13 (7)	*H. sapiens* (European)	186	135	130	104	95	110
Ofnet 24 (7)	*H. sapiens* (European)	184	131	140	100	95	114
Ofnet 6 (7)	*H. sapiens* (European)	183	137	140	97	92	106
Qafzeh 6 (7)	*H. sapiens* (Near East)	195	130	144	116	115	107
Skhul 4 (12)	*H. sapiens* (Near East)	206	128	148	110	105	132
Skhul 5 (12)	*H. sapiens* (Near East)	193	128	146	96	110	116
Skhul 9 (12)	*H. sapiens* (Near East)	213	130	145	115	106	120

All measurements are in millimeters. Ranges reported for recent modern human sample. Citations in parentheses indicate that those particular values were taken from the source specified.

Table S2. Coefficients of determination, regression slopes, and 95% confidence intervals for regressions of logged cranial measurements again logged geometric mean for the modern human comparative sample

Regressed variable	R^2	Major axis slope	95% C.I.	Reduced major axis slope	95% C.I.	Least squares slope	95% C.I.
ln GOL	0.665	1.24	1.21–1.27	1.19	1.17–1.22	0.973	0.946–1.00
ln BBH	0.558	1.52	1.48–1.56	1.37	1.34–1.40	1.03	0.989–1.06
ln XCB	0.287	1.65	1.57–1.74	1.32	1.28–1.36	0.707	0.663–0.750
ln BNL	0.758	1.54	1.51–1.57	1.46	1.44–1.48	1.27	1.24–1.30
ln BPL	0.494	1.96	1.90–2.03	1.63	1.59–1.67	1.15	1.10–1.19
ln ASB	0.433	1.53	1.48–1.59	1.33	1.30–1.36	0.876	0.837–0.915

Confidence intervals (C.I.) are bootstrapped for major axis and reduced major axis slopes. Note that similarity between regression slopes for a given measurement decreases as R^2 decreases.